

Dark-bright magneto-exciton mixing induced by Coulomb interaction in strained quantum wells

Y. D. Jho,^{1,3} F. V. Kyrychenko,¹ J. Kono,² X. Wei,³ S. A. Crooker,⁴

G. D. Sanders,¹ D. H. Reitze,¹ C. J. Stanton,¹ and G. S. Solomon⁵

¹*Department of Physics, University of Florida, Gainesville, FL 32611*

²*Department of Electrical and Computer Engineering, Rice University, Houston, TX 77005*

³*National High Magnetic Field Laboratory, Florida State University, Tallahassee, FL 32310*

⁴*National High Magnetic Field Laboratory, Los Alamos National Laboratory, Los Alamos, NM 87545*

⁵*Solid-State Laboratories, Stanford University, Stanford, CA 94305*

Coupled magneto-exciton states between allowed ('bright') and forbidden ('dark') transitions are found in absorption spectra of strained $\text{In}_{0.2}\text{Ga}_{0.8}\text{As}/\text{GaAs}$ quantum wells with increasing magnetic field up to 30 T. We find large (~ 10 meV) energy splittings in the mixed states. The observed anticrossing behavior is independent of polarization, and sensitive only to the parity of the quantum confined states. Detailed experimental and theoretical investigations indicate that the excitonic Coulomb interaction rather than valence band complexity is responsible for the splittings. In addition, we determine the spin composition of the mixed states.

PACS numbers: 78.20.Ls, 78.67.-n, 75.20.-g

When energy levels of excited states are tuned to the same energy, one can observe either crossing or anti-crossing behavior, depending on the coupling character of the external perturbations.¹ If the coupling matrix element of perturbing terms is non-vanishing, their corresponding wavefunctions are mixed so that the crossing is suppressed and replaced by anti-crossing behavior. In semiconductor heterostructures, valence-band complexity arising from spin-orbit coupling has been extensively investigated in GaAs-based quantum wells (QWs) and proposed as the main coupling mechanism.^{2,3,4,5,6,7} Due to the relatively small heavy-hole-light-hole (HH-LH) separation and resulting close proximity of valence band manifolds, the coupling of HH-LH exciton states in GaAs QWs can be substantiated through strong modifications of in-plane effective masses^{8,9} and transitions that are nominally forbidden in a simple two-band model can be observed optically.^{4,5,6,11} While a number of studies on valence-band complexity have been reported for exciton-mixing in QW's, it is conceivable that other mechanisms can also determine the nature of the interaction. Recently, anti-crossing involving bright and dark excitons in single quantum dot molecules due to coherent coupling between the states of the two dots has been observed.¹² In addition, large splittings of cyclotron resonance lines in $\text{Al}_x\text{Ga}_{1-x}\text{N}/\text{GaN}$ heterostructures have been reported¹⁰, indicating that the origins of anti-crossing interactions in high magnetic fields are not completely understood.

As a way to investigate whether exciton mixing is significantly influenced by other mechanisms, indium can be incorporated into the QW layer to induce strain. Since the lattice constant in $\text{In}_x\text{Ga}_{1-x}\text{As}$ QW is larger than that of surrounding GaAs layers, a biaxial compressive strain is introduced. The strain lowers the LH energy relative to the HH energy,¹³ thereby reducing the hole-level coupling and its corresponding repulsive interaction between LH and HH subbands.⁹ Thus, one can minimize the effects of valence band complexity in

$\text{In}_x\text{Ga}_{1-x}\text{As}$ QWs and obtain discrete optical spectra of HH and LH excitons in the high magnetic field regime. In addition, QWs provide lighter in-plane masses of HHs than that of LHs,^{7,14,15} thus magneto-exciton sublevels evolve differently in applied magnetic fields.^{3,8,16} Thus, $\text{In}_x\text{Ga}_{1-x}\text{As}/\text{GaAs}$ QWs are ideally suited for exploring the nature of the mixing interaction.

We report the observation of coupled states between forbidden and allowed interband transitions in strained $\text{In}_x\text{Ga}_{1-x}\text{As}$ QW structures in strong magnetic fields. A new kind of mixed magneto-exciton state is found in a system where the anti-crossing between hole states itself is suppressed. The samples, consisting of 15 layers of 8 nm thick QWs separated by 15 nm GaAs barriers, were grown by molecular beam epitaxy at 390 °C. To investigate the character of mixed states at low densities, absorption measurements were carried out in $\text{In}_{0.2}\text{Ga}_{0.8}\text{As}/\text{GaAs}$ multiple quantum wells for σ^- and σ^+ polarizations at 4.2 K. Magnetic fields perpendicular to the QW plane (Faraday geometry) were applied up to 30 T (45 T) using a resistive Bitter-type magnet (hybrid resistive-superconducting magnet) at 4.2 K. White-light from a tungsten-lamp was used as the excitation source. Both excitation and collection were performed through an optical fiber at normal incidence to the sample surface. In order to investigate exciton mixing at higher carrier densities, we also performed photoluminescence (PL) on our sample as a function of excitation power. For these experiments, a linearly polarized 150 fs, 775 nm pulse from a chirped pulse amplifier (Clark-MXR CPA-2001) was focused in free space to a 500 μm spot on the sample. Unpolarized PL was collected using an fiberoptic probe from the backside of the sample and examined as a function of both magnetic field and excitation power.

In order to specify a quantum well exciton state in a magnetic field, we use the high-field Landau notation (as opposed to the low-field excitonic notation); for low-field—high-field correspondence, see, e.g., ref.²¹. Each

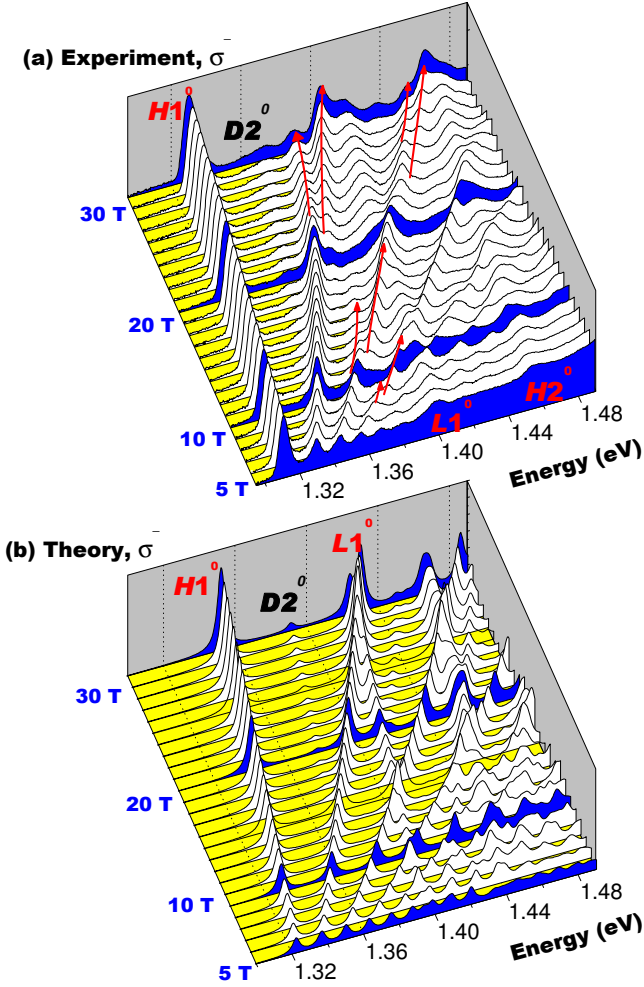


FIG. 1: (a) Experimental magneto-absorption spectra for $\text{In}_{0.2}\text{Ga}_{0.8}\text{As}/\text{GaAs}$ multiple quantum wells with σ^- polarization at 4.2 K for various fields up to 30 T. At zero field, three prominent peaks, indicated by $H1^0$, $L1^0$, and $H2^0$, are lowest HH exciton, lowest LH exciton, and second lowest HH exciton state, respectively. The lines $D2^0$ and $D2^1$ are assigned to the lowest and second lowest “dark” magneto-excitons associated with the $n_e = 1$ electrons and $n_h = 2$ heavy holes. The arrows are guides to the eye on separated magneto-exciton peaks. (b) Theoretical absorption spectra computed using an 8 band Pidgeon-Brown effective mass model. The dark state $D2^0$ is clearly visible in the spectra above 20 T.

state has four indices, i.e., N , M , n_e , and n_h (or n_l). Here N and M are electron and hole Landau quantum numbers, respectively ($N, M = 0, 1, 2, \dots$). The electron and HH (LH) QW energy levels are denoted by n_e and n_h (n_l). For the present work, the most relevant QW level indices are $n_e = 1$ and 2, $n_h = 1, 2$, and 3, and $n_l = 1$. For convenience, we are neglecting the spin index and center-of-mass momentum of each magneto-exciton state. In an ideal quantum well, interband transitions occur only when $N = M$ and $n_e = n_h$ (n_l). However, $n_e \neq n_h$ (n_l) transitions are usually weakly allowed in

real quantum wells due to perturbations such as strain, potential asymmetry, or valence-band mixing. We denote bright (i.e., optically active) HH (LH) exciton states $|N, M, n_e, n_h(n_l)\rangle = |N, N, n, n\rangle$ as Hn^N (Ln^N) and dark (i.e., optically inactive) HH exciton states $|N, M, n_e, n_h\rangle = |N, N, 1, n_h(n \neq 1)\rangle$ as Dn^N . Thus, all the dark states we are considering here are associated with $n_e = 1$ electrons; note also that the Landau quantum number is always conserved ($N = M$).

Figure 1(a) displays a series of representative absorption spectra as a function of magnetic field for the case of σ^- polarization. Note that at zero field, the HH and LH splitting is large (~ 100 meV) due to strain. As the field is increased, four effects are observed: (1) the absorption spectrum evolves from a step-like two-dimensional to a delta-function-like zero-dimensional density of states; (2) magneto-exciton levels are resolved up to $N = 6$ ($N = 2$) for the HH (LH) excitons; (3) the dark state $D2^N$ develops into a clearly resolved distinct peak; and (4) significantly, the $H1^N$ subbands with $N \geq 1$ split into two lines (indicated by the arrows in Fig. 1(a)). The energy at which the splitting occurs is found to be roughly the same distance below $L1^0$ for each state and is independent of polarization. The observation of the normally parity-forbidden $D2^0$ transition arises from the broken inversion symmetry in the presence of the magnetic field.

For comparison, Figure 1(b) shows results of a corresponding theoretical simulation based on an 8 band Pidgeon-Brown model^{17,18} of an undoped $\text{In}_{0.2}\text{Ga}_{0.8}\text{As}/\text{GaAs}$ superlattice on a GaAs substrate. Superlattice effects are obtained by finite differencing the 8 band Hamiltonian. While this model explicitly incorporates pseudomorphic strain in superlattice band-structure, excitonic effects resulting from the Coulomb interaction are not included. In these calculations, the conduction band offset is taken to be 0.7 of the total band offset and the strain in the wells is determined by the average lattice constant in the superlattice while the barrier lattice constant is pinned to the substrate lattice constant²⁵. To directly compare the experiments with a theory without Coulomb interaction, we display Fig. 1 only over the field range higher than 5 T. This theory reproduces the experimental features reasonably well, with one exception, namely that *there is no evidence of anti-crossing of the $H1^N - D3^0$ and $H1^N - D3^1$ states.*

Figure 2 (a) shows the prominent exciton lines obtained from fitting the experimental data in Figure 1 (a). The filled (hollow) circles are obtained from measurements with σ^+ (σ^-) polarizations. $H1^5$, $H1^6$, $L1^1$, and $L1^2$ are omitted for clarity although they were experimentally observed. In order to better visualize the data, the solid lines are simple parametric curves obtained using the reduced effective mass μ , the exciton binding energy E_X , and the QW energy gap as fitting parameters (neglecting spin splitting).²⁰ Two features are noteworthy. First, our data shows that H_3 is well separated and not coupled to L_1 . Thus, it should not acquire ‘bright’ character through valence-band mixing.^{5,11} In addition,

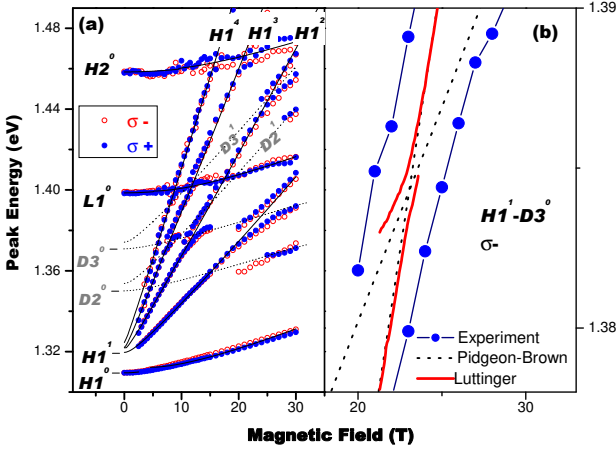


FIG. 2: (a) Magneto-exciton spectral line positions obtained by fitting absorption data for σ^+ (solid circles) and σ^- (hollow circles) from 0 to 30 T. The solid (dotted) lines depict the fitting curves of 2D magnet-exciton transitions for nominally allowed (forbidden) states. The $H1^5$, $H1^6$, $L1^1$, and $L1^2$ transitions are omitted for clarity. (b) A comparison of the experimental absorption spectrum for σ^- with theory at the $H1^1 - D3^0$ crossing point. The dotted line is computed from an 8 band Pidgeon-Brown effective mass theory without Coulomb interaction. The red line is calculated using a Luttinger Hamiltonian incorporating the Coulomb interaction.

the Landau subbands of $H1^N$ are split into two lines below (above) $L1^0$ exactly around the $D3^0$ ($D3^1$) energy position, while the more optically active $D2^0$ and $D2^1$ do not affect the $H1^N$ subbands. Therefore, the splitting is sensitive to the parity of the dark and bright exciton branches. Figure 2 (b) displays the $H1^1 - D3^0$ crossing point, comparing the experimental absorption data with theoretical predictions. Experimentally, we find a large (~ 9 meV) splitting in the energy of the states near 25 T. However, the Pidgeon-Brown model (dotted line) predicts no splitting *even though it incorporates full valence band complexity*. This is true for all $H1^N - D3^{N'}$ level crossings as well.

The failure of a model incorporating valence band complexity to explain these anti-crossings leads us to consider other mechanisms. There are two lines of evidence which suggest that the excitonic Coulomb interaction plays an important role in determining the splitting energies at the mixing points. First, we found that at high carrier densities the anti-crossing disappears. Figure 3 displays field-dependent magneto-photoluminescence (MPL) spectra upon excitation by 775 nm, 150 fs, 20 GW/cm² pulses from a high power chirped pulse amplifier (CPA). At these excitation powers, carrier density of 7.5×10^{12} cm⁻² are generated. The MPL spectra show various higher Landau-level states, but we do not observe any anti-crossing even though clearly resolved higher LL states are visible. This is consistent with the mixing having a Coulombic origin. At high densities, the Coulomb interaction is screened out, and excitonic states are replaced with magneto-plasmonic behavior.²³

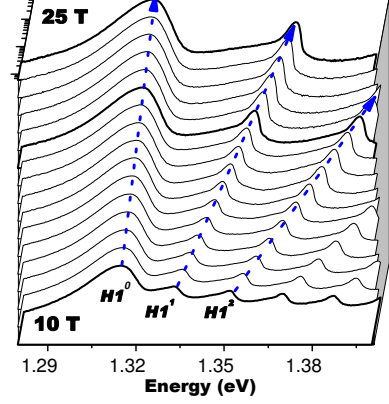


FIG. 3: Magneto-photoluminescence spectra obtained after excitation by high power femtosecond pulses. In contrast to the CW absorption spectra, no anti-crossing behavior is seen.

Second, when the excitonic Coulomb interaction is explicitly included in our calculations, we do observe anti-crossing behavior. We developed a comprehensive theory of magnetoexcitons in quantum wells. The theory is similar to that of Bauer and Ando³, but modified to be valid for high magnetic fields. For holes, our theory takes into account the Luttinger Hamiltonian in the axial approximation. The details of the calculations will be published elsewhere. The thick line in Figure 2 (b) presents the results of the Luttinger Hamiltonian for this system including the Coulomb interaction between electrons and holes. Our calculations show that Coulomb interaction do results in anticrossing of $H1^1$ and $D3^0$ states (Fig. 2b), however its magnitude (2 meV) is considerably smaller than the measured value of 9 meV.

While the Coulomb interaction is important in originating the anti-crossing, the large difference between the measured and theoretical energy splitting indicates that other mechanisms are also involved. We believe that the presence of uniaxial strain in the plane of the quantum well in our highly strained samples might play a crucial role. This strain breaks the rotational symmetry of the problem (which was used in our calculations) and this may substantially increase the magnitude of anti-crossing matrix elements

In addition to the optical character of the mixed states, our experiments also allow us to investigate how the mixed states ‘share’ their spin (g-factor) character. Near the anti-crossing point, the wavefunction ψ_{H1^N} mixes with $\psi_{D3^{N'}}$ to reveal a new set of wavefunctions:

$$\psi_1 = C_1 \psi_{D3^{N'}} + C_2 \psi_{H1^N} \quad (1)$$

$$\psi_2 = C_2 \psi_{D3^{N'}} - C_1 \psi_{H1^N}, \quad (2)$$

where coupling coefficients C_1 and C_2 , which are the functions of the Coulomb interaction potential $V_{N,N'}$, are normalized to unity ($C_1^2 + C_2^2 = 1$). Since $\psi_{D3^{N'}}$ is optically inactive, the optical character of the new states $\psi_{1,2}$

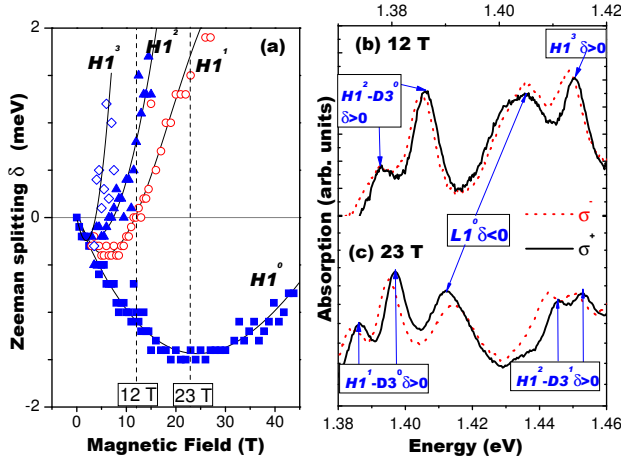


FIG. 4: (a) Field dependent Zeeman splitting for the $H1^N$ subbands. The solid lines are a guide to eye. At the fields denoted by dashed vertical line in (a), the individual σ^+ (solid lines) and σ^- (dotted lines) spectra are plotted for 12 T (b) and 23 T (c).

preserves the identity of ψ_{H1^N} by sharing its original oscillator strength. Hence, they are polarized in the same way. We can describe their polarization state by examining the Zeeman-splitting $\delta = E(\sigma^+) - E(\sigma^-) = -g_{ex}\mu_0 B$ between σ^+ and σ^- polarizations, where g_{ex} is the exciton g-factor and μ_0 is the Bohr magneton. g_{ex} is the sum of effective hole g-factor g_h , which consists of valence-band Luttinger parameters²⁴, and electron g-factor g_e .

Figure 4(a) shows measured δ for $H1^N$ transitions with N up to 3. The detailed shifts of δ for various coupled peaks are shown in Fig. 4(b) for 12 T and 4(c) 23 T. From Fig. 4(a), in all cases g_{ex} initially is negative and decreasing in value at low fields, reaching a minimum value and then increasing. Within a field range of 45 T,

$H1^N$ levels with $N \geq 1$ show a sign reversal of g_{ex} . The field at which the sign change occurs scales roughly inversely with sub-band index N . That the spin character of the dark states arises from their bright companion can be seen by comparing the $H1^N$, $D3^{N'}$, and $L1^0$ peaks in Figs. 4(b) and (c). For the three mixed branches (1) $H1^2 - D3^0$ [in Fig. 4(b)], (2) $H1^1 - D3^0$, and (3) $H1^2 - D3^1$ [in Fig. 4(c)], the sign of $\delta(g_{ex})$ for mixed states follow $H1^N$, regardless of the subband index (N , N'). In contrast, the light holes $L1^0$ shift in the opposite direction, and thus possessing the opposite sign of g_{ex} in both cases. This further indicates that the mixing is obtained without interference from the LH excitons.

In conclusion, we have presented a systematic study of mixed states of dark and bright magneto-excitons in strong magnetic field, wherein clear parity dependence was demonstrated. The polarization and parity dependence are understood through a Coulomb-interaction-mediated coupling between the same parity states as well as strain. Qualitative agreements were achieved on mixing strength and polarization dependence of mixed state. Field-dependent Zeeman splitting suggests that the spin character of the dark states comes from their bright exciton partners though the coupled states are linear combination of dark and bright excitons whose energy variations are redefined through off-diagonal matrix terms in the Luttinger Hamiltonian.

Acknowledgments

This work was supported by DARPA through Grant No. MDA972-00-1-0034, the NSF ITR program through grant DMR-032547, and the NHMFL In-house Science Program.

- ¹ T. G. Eck, L. L. Foldy, and H. Wieder, Phys. Rev. Lett. **10**, 239 (1963).
- ² L. Viña *et al.*, Phys. Rev. Lett. **58**, 832 (1987).
- ³ G. E. W. Bauer and T. Ando, Phys. Rev. B **38**, 6015 (1988), and references therein.
- ⁴ R. Magri and A. Zunger, Phys. Rev. B, **62**, 10364 (2000).
- ⁵ R. C. Miller *et al.*, Phys. Rev. B **32**, 8452 (1985).
- ⁶ L. W. Molenkamp *et al.*, Phys. Rev. B **38**, 6147 (1988).
- ⁷ G.D. Sanders and Y.C. Chang, Phys. Rev. B **32**, 5517 (1985); **35**, 1300 (1987).
- ⁸ L. Viña *et al.*, Phys. Rev. B **47**, 13926 (1993).
- ⁹ G. D. Sanders *et al.*, Phys. Rev. B **50**, 8539 (1994).
- ¹⁰ S. Syed, M. J. Manfra, Y. J. Wang, H. L. Stormer, and R. J. Molnar, Phys. Rev. B **67**, 241304 (2003).
- ¹¹ W.M. Theis *et al.*, Phys. Rev. B **39**, R1442 (1989).
- ¹² G. Ortner, M. Bayer, A. Larionow, V.B. Timofeev, A. Forchel, Y.B. Lyanda-Geller, T.L. Reinecke, P. Hawrylak, S. Fafard, and Z. Wasilewski, Phys. Rev. Lett. **90**, 86404 (2003).
- ¹³ K. F. Huang, K. Tai, S. N. G. Chu, and A. Y. Cho, Appl. Phys. Lett. **54**, 2026 (1989).

- ¹⁴ R.C. Miller, D.A. Keinman, W.T. Tsang, and A.C. Gosard, Phys. Rev. B **24**, 1134 (1981).
- ¹⁵ R.L. Greene, K.K. Bajaj, and E.E. Phelps, Phys. Rev. B **29**, 1807 (1984).
- ¹⁶ S.-R. Eric Yang and L.J. Sham, Phys. Rev. Lett. **58**, 2598 (1987).
- ¹⁷ C. K. Pidgeon and R. N. Brown, Phys. Rev. **146**, 575 (1966).
- ¹⁸ G. D. Sanders *et al.*, Phys. Rev. B **68**, 165202 (2003).
- ¹⁹ S.K. Cheung *et al.*, J. Appl. Phys. **81**, 497 (1997).
- ²⁰ O. Akimoto and H. Hasegawa, J. Phys. Soc. Jpn, **22**, 181 (1967).
- ²¹ A. H. MacDonald and D. S. Ritchie, Phys. Rev. B **33**, 8336 (1986).
- ²² G. Bastard, in *Wave mechanics applied to semiconductor heterostructures*, Paris: Éditions de Physique, p 317.
- ²³ L.V. Butov, V.D. Egorov, and V.D. Kulakovskii, Phys. Rev. B **46**, 15156 (1992).
- ²⁴ M. J. Snelling *et al.*, Phys. Rev B **45**, 3922 (1992).
- ²⁵ H. MuneKata, personal communication.